ELSEVIER

Journal of Nuclear Materials 241–243 (1997) 690–695

journal of nuclear materials

B2-Eirene modelling of ASDEX Upgrade

D.P. Coster [a,*], R. Schneider [a], J. Neuhauser [a], H.-S. Bosch [a], R. Wunderlich [a], C. Fuchs [a], F. Mast [a], A. Kallenbach [a], R. Dux [a], G. Becker [a], ASDEX Upgrade Team [a], B.J. Braams [b], D. Reiter [c]

[a] *Max-Planck Institut für Plasmaphysik, Garching, Germany*
[b] *Courant Institute, New York, USA*
[c] *Forschungszentrum Jülich (KFA), IPP, Jülich, Germany*

Abstract

The extension of the computational region of the coupled fluid plasma, Monte-Carlo neutrals code, B2-Eirene, to the plasma center is discussed. The simulation of completely detached H-mode plasma is presented, as is the modelling of He and Ne compression.

Keywords: ASDEX Upgrade; Fluid simulation; Monte-Carlo simulation; Edge localized modes; Helium exhaust and control

1. Introduction

This paper describes recent work done with, and enhancements to, the code package B2-Eirene [1,2]. (B2-Eirene is a coupling of the multi-species plasma fluid code, B2 [3,4], and the Monte-Carlo neutrals code, Eirene [5].)

The calculational domain for B2-Eirene has been extended from the usual 5–10 cm inside the separatrix all the way to the center (see Fig. 1). This was done to facilitate ELM modelling and the comparison with some diagnostics, and is described in Section 2.

In Section 3, neutral compression (the ratio of the neutral density close to the pump to the plasma density just inside the separatrix) and impurity enrichment (the ratio of the impurity compression to the deuterium compression) is modelled, and the results are compared to experimental results for helium and neon.

2. Linked core and scrape-off layer modelling

Recent work on B2-Eirene has allowed the use of deep grids that extend the domain of calculation from the usual scrape-off and divertor regions all the way into the core (see Fig. 1 for the geometry). The motivation for this work was to provide better core boundary conditions for ELM simulations [6,7], as well as a better basis for comparing simulated diagnostic signals from the code with experimental signals.

Others [8,9] have chosen to couple a core code to an edge code. Most of this work has concentrated on providing a better edge boundary condition for the 1-d core codes — our interest has been in simulating ELMs and we wanted a better core boundary condition for our edge code. It was thought that the position and nature of the 1-d/2-d transition might be too complicated for simulating ELMs and possibly MARFEs.

We use transport coefficients profiles (D, χ_e, χ_i, v_{conv}) as well as neutral beam heating and particle source profiles derived from the 1.5-d code, Baldur [10]. Exploration of various transport laws and their impact on the core plasma is probably best performed using fast 1- or 1.5-d codes; where our approach comes into its own, is when edge effects are important and have an impact on the core. For example, ELMs affect the edge strongly and the core to a lesser extent. With the grid extending all the way to the center we have a more realistic separatrix boundary condition than has been used in earlier simulations [6,7], and we can also investigate the effects of the ELMs on the core.

No problems were experienced when the same (small)

* Corresponding author. Tel.: +44-89 3299 1789; fax: +44-89 3299 2580; e-mail: dpc@ipp.mpg.de.

PII S0022-3115(96)00588-0

time-step was used in the core as in the edge. However the core introduces a new relaxation time into the problem, and trying to find an initial equilibrium profile (without ELMs) would take an inordinate length of time when using the same time-step everywhere. Therefore B2-Eirene was extended to allow different timesteps in different regions (core, scrape-off layer, inner and outer divertor). This introduced a new problem—taking larger timesteps in the core caused an unphysical spin up of the core. For the hydrogen only case, this was alleviated by adding an artificial parallel flow damping term in the core region. With impurities, though, this led to unphysical parallel gradients in the densities of the various species, leading to strange Z_{eff} profiles. Various approaches have been tried to alleviate this problem, including the use of a new, more accurate solver. Currently we use a combination of the parallel flow suppression factor and a term that equilibrates the individual charge state pressures along the field lines in the core by adding particle source and sink terms. These terms are only necessary when we want to increase the time-step in the core — if we use the same time-step dictated by the divertors, these terms are unnecessary.

In doing the ELM simulations, we have not tried to match any particular shot, but rather tried to match a regime of operation. On any particular shot, usually some key pieces of experimental information are missing.

A particular regime of recent interest on ASDEX Upgrade is the completely detached H-mode (CDH) [11]. In this regime, additional deuterium is added to the discharge to increase the divertor neutral density, and Ne is puffed in to increase the amount of radiation (both from near the outer midplane). Experimentally, the best results have been obtained when the D gas puff is feedback-controlled by the neutral gas pressure in the divertor, and the Ne gas puff by the amount of radiation as measured by the bolometers. During the CDH phase, the power reaching the plate drops significantly, and the type III ELMs which are observed do not burn through.

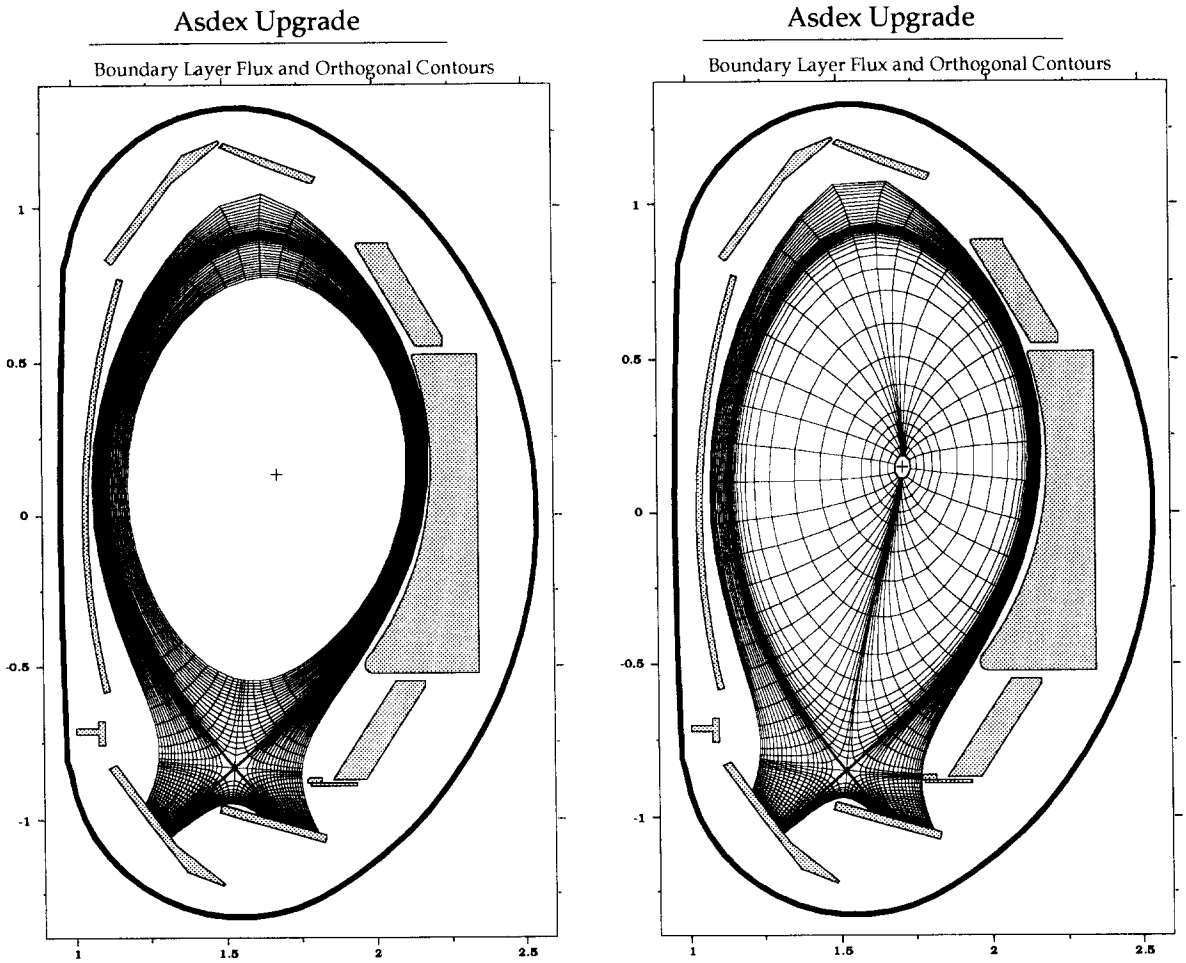

Fig. 1. Shallow and deep grids used to model ASDEX Upgrade. The shallow grid was used for the compression analyses, and the deep grid for the ELM calculations.

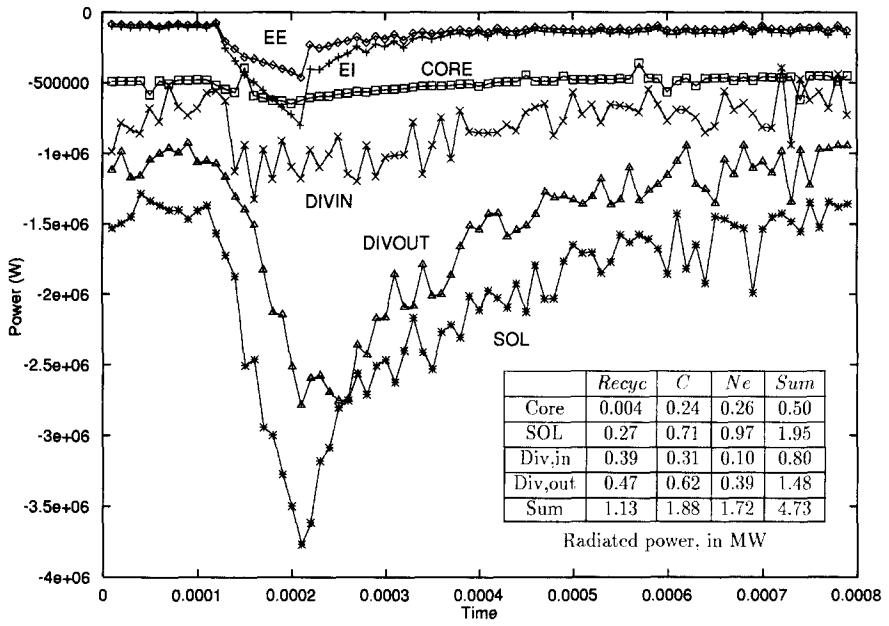

	Recyc	*C*	*Ne*	*Sum*
Core	0.004	0.24	0.26	0.50
SOL	0.27	0.71	0.97	1.95
Div,in	0.39	0.31	0.10	0.80
Div,out	0.47	0.62	0.39	1.48
Sum	1.13	1.88	1.72	4.73

Radiated power, in MW

Fig. 2. Simulation traces for one type III ELM event. The event occurs from 0.0001 s to 0.0002 s. The power radiated in the core (CORE) region (shallow grid), scrape-off layer (SOL), inboard divertor (DIVIN), outboard divertor (DIVOUT), and the power reaching the two divertors in the electron (EE) and ion (EI) channel are indicated.

This scenario on ASDEX Upgrade has been modelled, first with the usual shallow B2-Eirene grid [12], and more recently with the deep grid. In the code we reproduce the buffering effect of the radiating SOL and divertor, and see little power reaching the plate arising from the ELMs (Fig. 2). The deep grid was motivated by a mismatch in the predicted bolometer signals arising from the lack of a contribution from the core, as well as some peculiarities

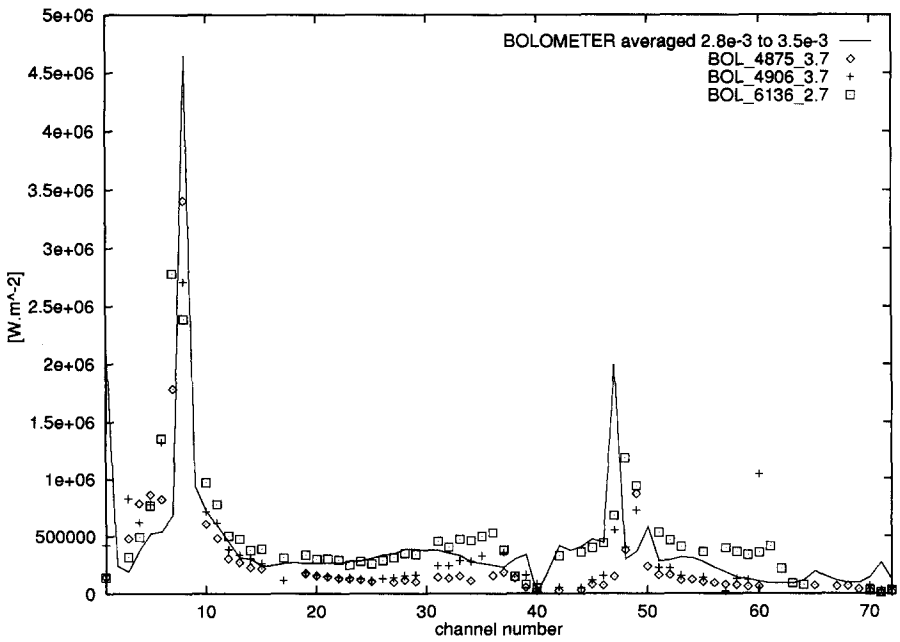

Fig. 3. Comparison of simulated bolometer signals with data from the experiment. The sight-lines of the various bolometer channels are given in Fig. 4. The three shots correspond to an un-puffed H-mode discharge (4875), a discharge with additional D puffing (4906), and a CDH discharge with combined Ne and D puffing (6136).

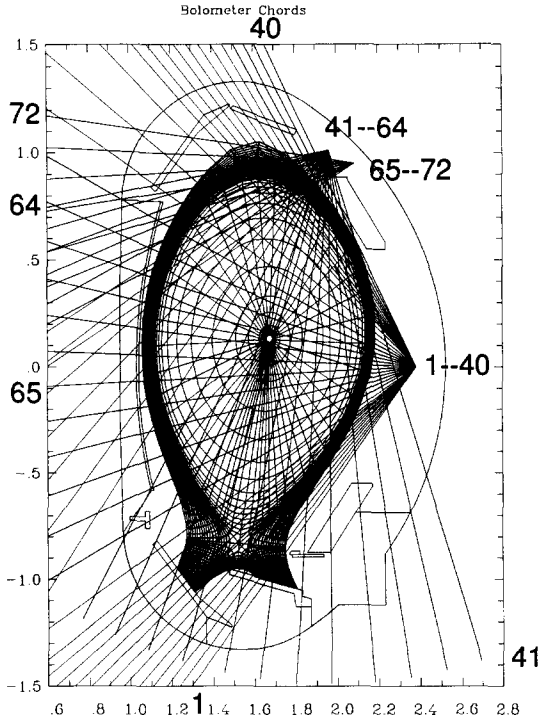

Fig. 4. Position of the Bolometer sight-lines used for Fig. 3.

introduced by the shallow grid interior boundary condition. We then moved to a deep grid (Fig. 3 shows the predicted bolometer signal compared to data from three different shots Fig. 4). In the initial runs, the core had not yet reached an equilibrium (which was not a critical problem in that it was the edge behavior that we were interested in, and the core merely provided an extended boundary condition to the edge region of interest). However, it was felt that to do 'an honest job',the core should also be relaxed to an equilibrium. It was at this point that we ran into the problems of core spin-up alluded to earlier, and further ELM calculations were put on hold until a solution could be found, a process that was further delayed by the interest in modelling impurity and working gas compression.

3. Modelling of compression

Compression is defined as the ratio of the neutral density of a particular species (D, He, Ne, etc.) measured close to the pumping duct to the plasma density of the same species close to the separatrix. The higher the compression, the faster the substance is pumped—enabling better feedback-control of the divertor density in the case of D, better feedback-control of the total radiation in the case of a recycling impurity such as Ne, and better exhaust of He, which, though not important for current machines, is critical for ITER.

Related work presented at this conference looks at the effect of various divertor geometries on ASDEX Upgrade [13], and compression of various impurities on the proposed Lyra configuration of ASDEX Upgrade [14].

For realistic modelling of compression, a comprehensive treatment of both the plasma and the neutrals is necessary. Since the pumping duct is usually some distance away from the plasma region, a way of modelling the neutrals in regions separate from the plasma is necessary. The Monte-Carlo treatment of the neutrals in B2-Eirene makes it possible to analyze the effects of different divertor geometries on impurities. Many simple 1-d treatments have looked at impurities in the divertor, but these all ignore important 2-d effects stemming from large scale flow patterns (see [15] and references therein). Some effort has also been put into using 2-d codes to model these impurity effects, though most of this has been done with simple fluid descriptions of the neutrals (see [16] for a recent overview). With these models, it is difficult to include the effects of physical structures lying outside the plasma computational domain (usually a grid aligned with the magnetic geometry).

In doing this work, B2-Eirene has been used to model D, C, Ne and He (in a few runs, Ar was used in place of Ne). The D, Ne (or Ar) and He densities were specified at the innermost surface of the shallow computational grid, and the C arose self-consistently from physical and chemical sputtering (see Fig. 1 for the geometry). The compression of the D, Ne (or Ar) and He was then calculated as the ratio of the neutral density in the pumping duct region to the average ion density in the core region. The experimental data (Fig. 5), found by looking at decay rates [17], reveals a fair amount of scatter when plotted as a function of the D flux at the pumping port, as well as some clear trends. Shown plotted on the same figure are some results from the B2-Eirene calculations.

Two effects are obvious when looking at the figure: (1)

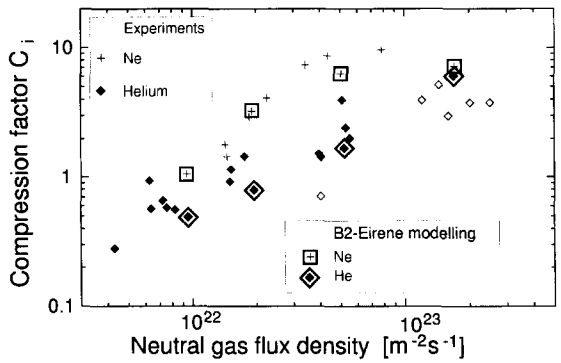

Fig. 5. Compression of helium and neon. The experimentally measured values for the compression of He and Ne for are plotted versus the neutral gas flux density measured in the pumping duct. B2-Eirene results for Ne and He are also plotted, surrounded by a square.

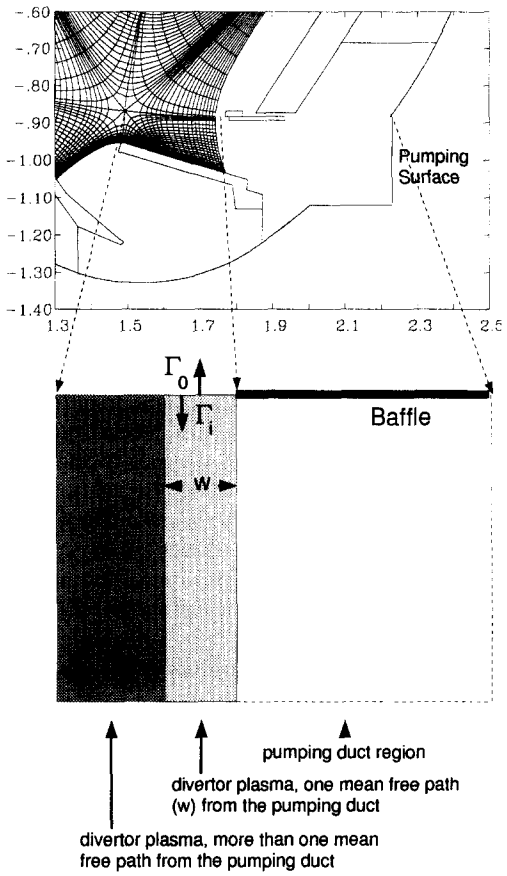

Fig. 6. Top: A small part of the computational region used. Bottom: An idealization of the outer part of the outer divertor. The model treats a small region one ionization mean free path deep connected on its right to the pumping duct, and above to the outer part of the SOL.

the increase in compression with increasing neutral gas density, and (2) the Ne compression being consistently higher than the He compression. The basic trends can be understood by considering a very simple model consisting of the outer edge of the outer divertor and the box formed by the pumping plenum and small baffle as shown in Fig. 6. We assume that this region is decoupled from the divertor region closer to the separatrix (see the later discussion).

The width w represents one ionization mean free path for neutrals arriving from the pump duct area. The fluxes marked Γ_0 and Γ_i are, respectively, the neutral flux passing out of, and the ion flux passing into, the region of interest. If we assume that the plasma velocity at this point, v_i is the same for all the species, and is determined by the D flux, then

$$\Gamma_i = v_i n_i w = v_D n_i w,$$

where n_i is the ion density at the entrance, and is assumed to be the same as the density further upstream (note this entrance is at the same level as the X-point).

$$\Gamma_0 = v_0 n_0 w,$$

where v_0 is the thermal velocity of the neutral, and n_0 is the density of the neutral in the pumping duct. Equating (assuming steady state, and feeding/losses only from the throat region), we get for the compression,

$$C = \frac{n_0^{\text{div}}}{n_i^{\text{main chamber}}} \approx \frac{n_0}{n_i} \approx \frac{v_i}{v_0}.$$

The flux density used for the ordinate of the compression graph is $n_0 v_0$ evaluated for D, and this equals $n_i v_D$ based on the D in the throat region. Thus an increase in the ordinate corresponds to an increase in this product: the n_i should not vary too much, since the width is determined by the ionization mean free path, w, and increasing density will only decrease w, lowering the average density over w. Thus the strongest effect comes from increasing v_D. This, then explains the increase in compression with increasing deuterium flux density. The higher Ne compression in

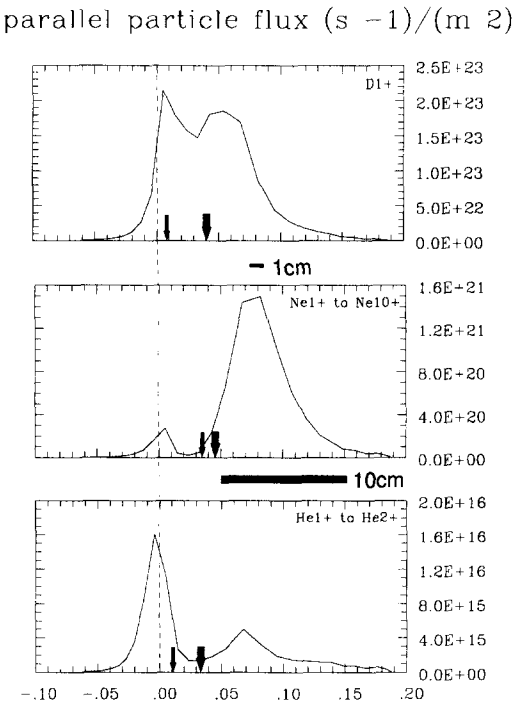

Fig. 7. The fluxes of D, Ne and He to the outer divertor plate are plotted as a function of position (in m) along the divertor plate. Zero corresponds to the position of the separatrix. The arrows show the positions of the 1 cm (thin arrow) and 10 cm (thick arrow) ionization mean free path points (calculated using local values at the plate). For the Ne case, the smaller peak to the left of the two arrows does not communicate directly with the pump duct (which is to the right), while the right, higher peak does.

comparison to He is partly explained by the lower v_0 for Ne.

This simple model has assumed we can separate out a region on the outside that is not coupled to the particle flux at the separatrix, and that is only fed from above. In reality, some feeding will also occur from the left (as well as some losses to the left), and the higher He ionization mean free path will play a role. Also important, and not included in this simple model, is the varying width of the modelled area depending on species, as well as such effects as charge exchange. Another important player in determining the exact flow patterns of the impurities is the presence of flow reversal zones, and the position of the ionization front for the particular species with respect to the position of the flow reversal zones. All these effects are in B2-Eirene, and determine the details seen in the compression plot. Fig. 7 shows one such subtlety — the parallel particle flux densities reaching the outer target plate are plotted as a function of position along the plate. Comparing the Ne and He plots, we see a significant secondary peak (on the right, away from the separatrix) in the Ne flux, whereas the He flux shows only a smaller secondary flux. This is probably driven by the shorter Ne ionization mean free path (the point at which this equals 1 cm based on plate densities and temperatures is well separated from the separatrix for Ne, whereas it is only 1 cm away from the separatrix for He).

4. Conclusions

An extension of the B2-Eirene computational region all the way to the center of the plasma is presented, and some of its features are discussed. The experimentally observed disappearance of the heat flux to the target during the completely detached H-mode (CDH) is reproduced in the B2-Eirene simulations, and is shown to arise from the buffering effect of the impurities, whose radiation increases during and after the ELM event. The experimentally observed behavior of compression versus neutral flux density in the divertor pump duct is reproduced by B2-Eirene modelling, and a simple model is presented explaining the main features.

References

[1] R. Schneider, D. Reiter, H.P. Zehrfeld, B. Braams, M. Baelmans et al., J. Nucl. Mater. 196–198 (1992) 810.
[2] D. Reiter, J. Nucl. Mater. 196–198 (1992) 80.
[3] B.J. Braams, Computational Studies in Tokamak Equilibrium and Transport, PhD thesis, Rijksuniversiteit, Utrecht, Nederland (1986).
[4] B.J. Braams, Technical Report 68, Next European Torus (1987).
[5] D. Reiter et al., J. Nucl. Mater. 220–222 (1995) 987, PSI 94 Mito.
[6] D. Coster, B. Braams, J. Neuhauser, D. Reiter, R. Schneider et al., in: Europ. Physical Soc. Conf. on Controlled Fusion and Plasma Physics, Vol. 18, Montpellier (1994) pp. 846–849.
[7] D. Coster, R. Schneider, J. Neuhauser, G. Becker, H.-S. Bosch et al., in: Bulletin of the American Physical Society (Liousville, KY, 1995).
[8] M. Baelmans, D. Reiter, M. Tokar and Börner, Consistent Core-Edge Plasma Modelling for TEXTOR Plasmas with Carbon Impurities, Presented at the 5th Workshop on Plasma Edge Theory, December 1995, Asilomar, CA (1996).
[9] A. Tarditi, R. Cohen, G. Craddock, J. Crotinger, T. Rognlien et al., Contrib. Plasma Phys. 36 (1996) 132, 5th Workshop on Plasma Edge Theory, December 1995, Asilomar, CA.
[10] G. Becker, H. Fahrbach, J. Fuchs, O. Gehre, J. Gernhardt et al., in: Europ. Physical Soc. Conf. on Controlled Fusion and Plasma Physics, Vol. 19C I (Bournemouth, 1995) pp. 25–27.
[11] O. Gruber et al., Phys. Rev. Lett. 74 (1995) 4217.
[12] R. Schneider et al., in: Europ. Physical Soc. Conf. on Controlled Fusion and Plasma Physics, Vol. IV (Bournemouth, 1995) pp. 285–288.
[13] H.-S. Bosch et al., these Proceedings, p. 82.
[14] R. Schneider, H. Bosch, J. Neuhauser, D. Coster, K. Lackner et al., Divertor Geometry Optimization for ASDEX Upgrade, this conference (1996).
[15] P. Stangeby and J. Elder, Nucl. Fusion 35 (1995) 1391.
[16] A. Loarte, these Proceedings, p. 118.
[17] H.-S. Bosch et al., Particle exhaust studies in ASDEX Upgrade, to be submitted.